The Tubulin-Bound Conformation of Paclitaxel: T-Taxol vs "PTX-NY"†

Yutao Yang, Ana A. Alcaraz, and James P. Snyder*

Department of Chemistry, Emory University, Atlanta, Georgia 30322

Received October 19, 2008

Nearly 35 years after its discovery and 11 years after FDA approval of paclitaxel (PTX) as a breakthrough anticancer drug, the 3-D structure of the agent bound to its β-tubulin target was proposed to be T-Taxol. The latter bioactive form has recently been challenged by the Ojima group with a structure, "PTX-NY" ("REDOR Taxol"), in which the C-13 side chain is proposed to adopt a different conformation and an alternative hydrogen-bonding pattern in the tubulin binding site. Previously, the two conformers were compared to show that only T-Taxol fits the PTX-derived electron crystallographic density. That work has been extended by molecular mechanics and quantum chemical methods to reveal that the PTX-NY conformation is relatively less stable, on average, by 10−11 kcal/mol. In agreement with NMR studies, an 11 ns molecular dynamics treatment for PTX in an explicit water pool locates T-Taxol along the trajectory, but not PTX-NY. Docking of various PTX conformers into the electron crystallographic binding site of tubulin demonstrates that PTX-NY cannot be accommodated unless the pocket is reorganized in violation of the experimental constraints. Finally, analysis of the structures of T-Taxol and PTX-NY for their capacity to predict the existence of superpotent PTX analogues discloses that only the former forecasts such analogues, as now established by the T-Taxol-inspired synthesis of bridged taxanes. In sum, all empirical criteria support T-Taxol as the bound conformation of PTX on β-tubulin in microtubules.

Paclitaxel (**1**, PTX), a complex diterpene biosynthesized by the bark and leaves of the Pacific yew tree (*Taxus brevifolia*), was discovered to be a potent anticarcinogen in an early NCI natural product screening program in 1967.[1] The compound's constitution,[2] mechanism of action as a disrupter of microtubule dynamics,[3] and 3-D structure[4,5] were determined 4, 8, and 28 years later, respectively. In 1992, 25 years after discovery, the compound won FDA approval for treatment of late-stage ovarian and breast cancer.[6] Though the source of considerable toxicity[7] and subject to resistance in cells[8] and in the clinic,[9] PTX became a billion dollar drug[10] and served as a life-extender for many afflicted with cancer.

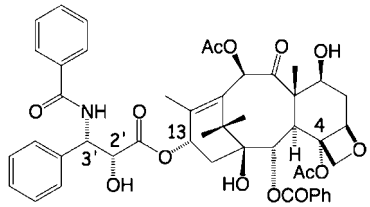

1

Throughout the long path from discovery to clinic, the bioactive conformation of PTX bound to microtubules remained elusive. Several photoaffinity labeling studies determined the β-tubulin subunit to be the target,[11] while a landmark electron crystallographic (EC) investigation of the tubulin dimer structure in Zn^{2+} and PTX stabilized sheets provided a low-resolution snapshot of the drug's binding site.[12,13] In 2001, two subsequent reports refined the ligand binding site to reveal a novel PTX conformation[14,15] christened "T-Taxol".[15] Given the uncertainties in the EC resolution (3.5 Å), it was necessary to confirm the bound ligand structure independently. Examination of the proposed bioactive conformation indicated rather close contact between the C-4 acetate methyl group and the *ortho* and *meta* positions of the phenyl ring at C-3′. A series of taxanes was designed to bridge these centers so as to lock the taxane skeleton into the T-Taxol conformation. Subsequently synthesized and assayed for cytotoxicity, the analogues with short bridges linked to the *ortho*-C-3′ position proved to be 20−50-fold more active than parent PTX.[16−18] In contrast to the conformational ensembles of the latter,[19] the conformations of the bridged compounds proved to dominate in solution as the T-Taxol form.[16,17] Subsequently, the Gif-sur-Yvette group employed the T-Taxol structure to devise a novel and active bridged taxane,[20] while careful multidisciplinary REDOR NMR studies of tubulin−PTX complexes have confirmed essential interatomic distances for the proposed binding conformation.[21]

In spite of these successes, the T-Taxol conformation has been challenged by the Stony Brook group as being disfavored relative to another conformation in which the C-13 side chain adopts a spatial orientation that permits a buried hydrogen bond between the C-2′ OH and His227.[22,23] We take note of the fact that the latter conformer has been named "REDOR-Taxol" as an indication that the structure conforms to the REDOR-determined interatomic distances measured by the Schaefer group.[21] However, not only does T-Taxol likewise meet these geometric constraints,[21] but many other PTX conformations do as well.[24] Thus, there are a multitude of REDOR-Taxols including T-Taxol. When referring to one of these, it seems to us appropriate to differentiate. For this reason, we will use PTX-NY to refer to the REDOR structure proposed by the New York-based Stony Brook group.

In previous reports, we compared the two conformations in question with respect to their abilities to match the densities derived from the electron crystallographic study that provided the structure of the tubulin dimer complexed with PTX.[12] Not only is T-Taxol unique in threading the C-13 side chain through the experimental density as depicted by $2F_{obs} - F_{calc}$ omit maps, but difference maps reveal that the PTX-NY structure docked into the tubulin binding site leads to incorrectly filled density.[21a,24,25] The purpose of the present work is to extend the comparison of the T-Taxol and PTX-NY structures in order to examine more comprehensively which is a more suitable model for the bioactive conformation of PTX in β-tubulin.

An anonymous reviewer of the studies described below has written, "Unfortunately, a lot of what has been said on this topic consists of these groups talking past each other because they employ quite different methodologies.... (This work) is not likely to persuade

† Dedicated to Dr. David G. I. Kingston of Virginia Polytechnic Institute and State University for his pioneering work on bioactive natural products.

* To whom correspondence should be addressed. (J.P.S.) Tel: (404) 727-2415. Fax: (404) 727-6586. E-mail: jsnyder@emory.edu.

10.1021/np800662j CCC: $40.75
Published on Web 03/06/2009

Table 1. Relative MMFFs and OPLS-2005 Molecular Mechanics Energies of the Torsion-Constrained and Geometry-Optimized T-Taxol and PTX-NY C-13 Side Chains Represented by Methyl Ester **5**; GBSA/H_2O Continuum Solvation Model

force field	T-Taxol, kJ/mol	PTX-NY, kJ/mol	ΔE, kcal/mol
MMFFs	233.8	253.3	4.7
OPLS-2005	−69.1	−36.7	7.8

people who already have an opinion about the bound state conformation of Taxol." On the contrary, the structure of paclitaxel bound to β-tubulin is not a matter of opinion. At the microscopic level, there is one specific conformation of the molecule in complex with the tubulin dimer in microtubules. In the present investigation, we address key questions comparatively in order to judge the merits of the proposals and to identify that specific molecular shape. The lines of evidence available in the present case are 3-fold and include both experimental and computational data: (1) a refined 3.5 Å resolution electron crystallographic structure of bound PTX, (2) bridged PTX analogues that constrain the C-13 side chain to a limited number of conformations, and (3) structural and computational analyses. The latter involve small-molecule methods refined over the years to provide high to moderate accuracy as it pertains to molecular structure: conformational analysis, relative energy evaluation, molecular dynamics simulation, and prediction of ligand poses in protein binding sites. All of these tools are employed for **1** and the highly active bridged analogues **2** and **3**. We demonstrate that the T-Taxol conformation is superior in each frame of reference.

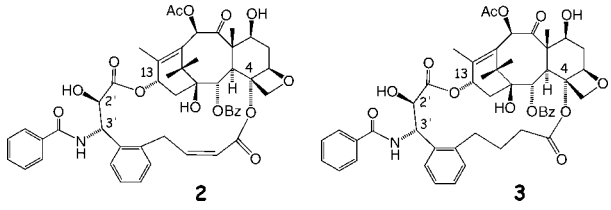

2 **3**

Results and Discussion

To initiate the discussion, the origins of the T-Taxol and PTX-NY conformations as the bioactive conformation of PTX on β-tubulin will be reviewed, and the supporting experimental data will be highlighted. The T-Taxol form was first identified (though not yet named) as a low-population (4%) member of an ensemble of PTX conformations in $CDCl_3$.[26] Three years later, it was also detected as a 2% contributor to the conformational equilibrium of a water-soluble taxane in D_2O/DMSO-d_6.[19] These solution conformations along with other rotational isomers derived from taxane X-ray crystal structures (a total of 26) were viewed as empirical data points on paclitaxel's torsional energy surface and, therefore, regarded as candidates for the bioactive form of the ligand at the photolabeled β-tubulin binding site. Given the low-resolution EC structure of the protein, this approach was taken to avoid the ambiguities of computationally based *de novo* ligand docking and to proceed with PTX structures having independent existence outside the computer. Each was subsequently docked into the experimental density map of the tubulin−PTX complex derived from an EC analysis of the tubulin dimer in PTX and Zn^{2+} stabilized sheets (pdb code 1TUB).[12] The best fit to the EC density, an NMR structure, also satisfied the available and subsequent REDOR NMR solid-state distances.[21] The bioactive conformer was christened T-Taxol in 2001.[15] A closely related structure that overlaps the latter reasonably well (see Conclusions) but does not match the REDOR interatomic separations within error limits[21a,24] was simultaneously derived by refinement of the 3.5 Å resolution tubulin dimer structure (pdb code 1JFF[14]).

The origin of the PTX-NY conformer is based on a more limited effort to identify a PTX geometry consistent with two REDOR-determined interatomic distances.[21b] The latter were employed as constraints in an *in vacuo* Monte Carlo MM3* conformational search for fluorinated 2-FB-PT, **4**, with a 12 kcal/mol energy cutoff.[22]

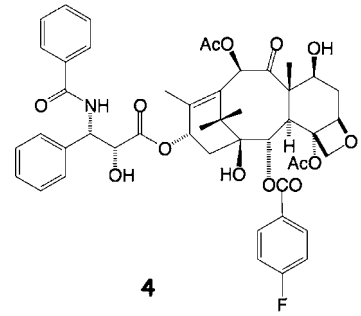

4

The resulting 1371 conformers were clustered to give 16 subsets of structures represented by a single cluster member without regard to relative energy. Each of the 16 structures was docked into the unrefined tubulin−PTX complex (1TUB)[12] by a two-step minimization procedure to produce protein−ligand binding site models that appear to have been altered significantly from the geometry determined by electron crystallography.[12,14,15] Although none of the PTX models strictly maintained the two interatomic distances determined by REDOR, the model that deviated least was selected as PTX-NY ("REDOR-taxol") in 2005.

The experimental data supporting proposals for the two conformers are readily summarized. PTX-NY closely matches two REDOR NMR interatomic distances and subsequently several others.[21] However, no attention was devoted to assuring that the structure resides among low-energy conformers that meet the distance criteria. By contrast, T-Taxol was selected from two dozen experimental conformations within 2−3 kcal/mol of either solid-state or solution global minima. The conformer satisfies both the EC density of the tubulin−PTX complex[12] and the REDOR NMR distances.[21]

The original proposal for NY-PTX included an *in vacuo* CVFF force field calculation of the energy relative to T-Taxol suggesting PTX-NY to be more stable by ~10 kcal/mol.[22] Since the CVFF energy difference was dominated by torsional terms and the method is not highly parametrized for small molecules, it seemed prudent to reevaluate the energetics with methods tailored to organic architectures and capable of incorporating an estimate for solvent effects. Subsequent sections address this and other issues in several ways.

Relative Energies of the T-Taxol and PTX-NY C-13 Side Chains. The structural difference between T-Taxol and PTX-NY resides primarily in the C-1′ to C-3′ sector of the C-13 side chain of paclitaxel. For the parent PTX molecule (**1**), we have compared the energies of the two C-13 side chain conformations in three independent structural contexts and theoretical frameworks. First, the side chain was represented as the methyl ester **5**. Each of the two conformers in question was frozen torsionally on the optimized energy surfaces of two of the currently most reliable force fields for small molecules (MMFFs and OPLS-2005; all bond distances and bond angles were relaxed). The PTX-NY conformer is suggested to reside 5−8 kcal/mol higher in energy (Table 1).

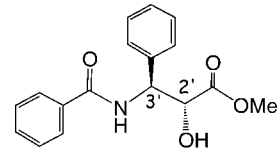

5

Second, to ensure that both conformations are energy minima on these surfaces, we performed thorough conformational searches with the same two force fields including full geometry optimization followed by ROCS 3D searching[27] of the conformational ensembles to locate the T-Taxol and PTX-NY structures. Both are either local

Table 2. Single-Point Quantum Chemical Calculations on the OPLS-2005 Constrained-Optimized T-Taxol and PTX-NY C-13 Side Chains **5**

model	PTX-NY, au	T-Taxol, au	E(NY) − E(T),[a] au	E(NY) − E(T),[a] kcal/mol
HF/6-31G*	−1007.558830	−1007.573941	0.015111	9.5
HF/6-311G*	−1007.762566	−1007.778154	0.015587	9.8
HF/6-311+G*	−1007.780290	−1007.795612	0.015321	9.6
B3LYP/6-31G*	−1013.686174	−1013.699795	0.013621	8.5
B3LYP/6-311G*	−1013.924903	−1013.939159	0.014255	8.9
B3LYP/6-311+G*	−1013.946069	−1013.959463	0.013394	8.4
MP2/6-31G*	−1007.558872	−1007.573967	0.015094	9.5
MP2/6-311G*	−1007.762580	−1007.778172	0.015592	9.8
MP2/6-311+G*	−1007.780290	−1007.795614	0.015323	9.6

[a] NY = PTX-NY and T = T-Taxol conformations.

Table 3. T-Taxol and PTX-NY Structures Constrained to the Original C-13 Side Chain Torsional Angles and Geometry Optimized with Molecular Mechanics Methods

force field	PTX-NY, kJ/mol	T-Taxol, kJ/mol	ΔE, kJ/mol	ΔE, kcal/mol
MM2	543.6	508.4	35.2	8.4
MMFFs	936.3	891.0	45.3	10.8
OPLS-2001	275.8	223.8	52.0	12.4
OPLS-2005	135.2	74.4	60.8	14.5
OPLS-2005/ MMFFs[a]	937.2	894.4	42.8	10.2

[a] Constraint optimized sequentially with OPLS-2005 followed by MMFFs.

Table 4. T-Taxol and PTX-NY Conformations Geometry Optimized without Constraints to the Nearest Local Minima with Molecular Mechanics Methods

force field	PTX-NY, kJ/mol	T-Taxol, kJ/mol	ΔE, kJ/mol	ΔE, kcal/mol
MM2	496.6	485.5	11.1	2.7
MMFFs	901.2	867.0	34.2	8.2
OPLS-2001	220.6	207.3	13.3	3.2
OPLS-2005	73.8	52.8	21.0	5.0

or global minima depending on the force field (see Experimental Section). Relaxed PTX-NY is again evaluated at 5−8 kcal/mol higher in energy than T-Taxol.

Third, the two OPLS-2005 frozen conformers have been subjected to nine single-point quantum chemical energy evaluations with the HF, DFT (B3LYP), and MP2 models (Table 2). Each was evaluated with both double- and triple-ζ basis sets including both heavy atom polarization and diffuse functions. Once again, the PTX-NY conformer is found to be less stable than the T-Taxol form by 8.5−9.8 kcal/mol.

Consequently, from the point of view of the C-13 side chain alone, the strain energy penalty paid by the PTX-NY ligand upon binding to tubulin is in the 5−10 kcal/mol range relative to T-Taxol. We were interested to learn if this rather high expenditure carries over to the full PTX molecule.

Relative Energies for Full-Molecule PTX Conformations. Force field optimization was performed both with and without torsional constraints on all atoms of the two PTX conformers under consideration here. The constrained dihedral angle calculations utilized the published side chain conformations[15,22,23] and five force fields or combinations of them (Table 3). The unrestrained calculations employed four of the same methods (Table 4). Energy differences once again posit PTX-NY to be less stable than T-Taxol by 3−15 kcal/mol. Single-point quantum chemical energies were obtained on the OPLS-2005/MMFFs pair of constrained geometries using the B3LYP density functional and three reliable basis sets (Table 5). Consistently, T-Taxol proves more stable than PTX-NY by 15−16 kcal/mol.

It appears that the C-13 side chain is a reasonable conformational surrogate for the full paclitaxel molecule with the exception that it can underestimate the relative stability of T-Taxol in comparison to PTX-NY. Quite apart from any reorganization of the tubulin amino acid side chains in the taxane binding pocket upon complexation of the protein by the latter, the required ligand strain energy is extraordinary. Both issues are discussed in more detail in subsequent sections.

Highly Active Bridged Taxanes. Numerous attempts have been made to produce bridged taxanes that mimic the bioactive conformation of paclitaxel on β-tubulin. For such a complex molecule and bridges of varying length, complete conformational locking is not possible. However, rather efficient conformational restriction can be introduced in this way and confirmed by NMR.[16,17] Worldwide efforts directed at constructing internal bridges in PTX have been reviewed recently.[28] While judicious choice of substituents can produce unbridged taxanes with activities superior to parent PTX,[29] only one bridging strategy has achieved this outcome, namely, two carbon bridges between the methyl group of the acetate at C-4 and the *ortho*-position of the phenyl moiety at C-3′ in **1**.[16−18]

Compounds **2** and **3** represent the principle and have proved to be 20−50-fold more cytotoxic than PTX against several cell lines, as do their analogues. Obviously, any PTX C-13 side chain conformation that is proposed as the bioactive conformation needs to accommodate such structures as well. In this spirit, we have generated the corresponding PTX-NY conformations and compared them to the previously published T-Taxol forms.[16−18] Tables 6 and 7 summarize the results of five force field approaches for both structures.

In this framework, the PTX-NY geometry is predicted to exist as an unstable conformer at 7−28 and 6−10 kcal/mol for **2** and **3**, respectively, above the corresponding T-Taxol form depending on the method of energy evaluation. To obtain an alternative comparison, we have computed the single-point and geometry-optimized energy differences for both conformations at the B3LYP/6-31G* level of theory (Table 8). The single-point energy differences parallel those from the molecular mechanics estimates; the $\Delta\Delta E$ values for PTX-NY-**2** and PTX-NY-**3** are 28 and 7 kcal/mol, respectively, higher than the corresponding T-Taxol conformers. Geometry optimization with B3LYP/6-31G* leads to 7 kcal/mol destabilization for PTX-NY-**2**, while PTX-NY-**3** proved to be an unstable entity on the DFT energy surface (see Experimental Section).

As a result, the polycyclic bridged PTX analogues provide no relief for the PTX-NY conformer. In fact, it would seem that the unsaturated analogue **2** raises the energy difference between the two conformations drastically. This is not surprising considering the observation that bridging between the C-4 acetate and C-3′ phenyl ring increases the solution concentration of T-forms from 2−5% to 40−80% populations.[16,17] In none of the latter NMR conformational deconvolution analyses are the PTX-NY conformations observed.

Conformational Differences between T-Taxol and PTX-NY. Why is it that a palette of both molecular mechanics and quantum chemical methods predict that the PTX-NY conformation is consistently 6−28 kcal/mol higher in energy than the T-Taxol

Table 5. Single-Point Quantum Chemical Energies for T-Taxol and PTX-NY Conformations Torsion-Constraint-Optimized with OPLS-2005/MMFFs

model	PTX-NY, au	T-Taxol, au	E(NY) − E(T),[a] au	E(NY) − E(T),[a] kcal/mol
B3LYP/6-31G*	−2929.501663	−2929.527763	0.026100	16.4
B3LYP/6-311G*	−2930.188739	−2930.213795	0.025057	15.7
B3LYP/6-311+G*	−2930.238158	−2930.263956	0.025798	16.2

[a] NY = PTX-NY and T = T-Taxol conformations.

Table 6. T-Taxol-**2** and PTX-NY-**2** Geometry Optimized without Constraints Using Molecular Mechanics Methods

force field	T-Taxol-**2**, kJ/mol	PTX-NY-**2**, kJ/mol	ΔE, kJ/mol	ΔE, kcal/mol
MM3	787.8	816.8	29	6.9
MMFFs	988.5	1036.2	47.7	11.4
OPLS-2005	85.2	204.0	118.8	28.4
OPLS-2005/MM3[a]	752.5	815.8	63.3	15.1
OPLS-2005/MMFFs [a]	945.6	1031.9	86.3	20.6

[a] Optimized sequentially with OPLS-2005 followed by either MM3 or MMFFs.

Table 7. T-Taxol-**3** and PTX-NY-**3** Geometry Optimized without Constraints Using Molecular Mechanics Methods

force field	T-Taxol-**3**, kJ/mol	PTX-NY-**3**, kJ/mol	ΔE (kJ/mol)	ΔE (kcal/mol)
MM3	711.3	753.6	42.3	10.1
MMFFs	914.2	944.9	30.7	7.3
OPLS-2005	72.7	112.5	39.8	9.5
OPLS-2005/MM3[a]	712.4	748.7	36.3	8.7
OPLS-2005/MMFFs[a]	914.6	939.1	24.5	5.9

[a] Optimized sequentially with OPLS-2005 followed by either MM3 or MMFFs.

Table 8. Single-Point (sp) B3LYP/6-31G* Quantum Chemical Energies for **2** and **3** in T-Taxol and PTX-NY Conformations Optimized with OPLS-2005/MMFFs; B3LYP/6-31G* Optimized Geometries (opt)[a]

		T-Taxol, au	PTX-NY, au	E(NY) − E(T),[b] au	E(NY) − E(T)[a,b] kcal/mol
2	sp	−3005.716643	−3005.672321	0.044321	28.3
2	opt	−3005.750762	−3005.740299	0.010463	6.6
3	sp	−3006.944942	−3006.934127	0.010815	6.8
3	opt[c]	−3006.980195			

[a] sp = single point, opt = optimized. [b] NY = PTX-NY and T = T-Taxol conformations. [c] Unconstrained optimization of **3** as PTX-NY did not retain the conformation, but led to a structure in which the C-13 side chain falls near the average of T and NY forms.

conformer when structures **1**−**3** and **5** are evaluated? Figure 1 provides two comparative views of the C-13 side chains of T-Taxol and PTX-NY that illuminate some of the key differences. Looking down the T-Taxol C2′−C1′ bond in a Newman sense in Figure 1a highlights that the C2′−OH and C1′═O are staggered but linked by a hydrogen bond. Figure 1c illustrates the point in a side view.

Importantly, the PTX-NY conformer incorporates a repulsive O---O interaction between the C2′-OH and ester oxygens (Figures 1b and 1d). At a distance of 2.7 Å, the separation is 0.3 Å below the sum of the van der Waals radii (O: 1.52 Å[30]). This feature is most likely a dominant contributor to the relatively high energy of the structure.

In addition, the reader will notice that the conformations differ by an approximate 165° rotation around the C2′−C1′ bond. This can be seen in Figure 1, in which the C-3′ terminal phenyl groups spin counterclockwise around the latter bond from Figure 1a to Figure 1b. Obviously, the C3′−C2′ backbone bond likewise participates in the change. The significant positional displacement of the C-13 terminal aromatic rings from the T- to the NY-form has implications for the bioactive binding pose in β-tubulin. In the docking section below, we take up this point further.

Molecular Dynamics of PTX in Water to Locate the T-Taxol and PTX-NY Conformations. Since a variety of well-established computational methods suggest that PTX-NY is 10−11 kcal/mol less stable than the T-Taxol conformer on average, we were interested in knowing if the dynamic behavior of the molecule in a box of explicit water molecules might create a more favorable energy balance. Ojima and colleagues have suggested that PTX-NY enjoys "a very buried H bond of increased strength" to His227 in tubulin.[22] Constant contact with water molecules able to engage in such a hydrogen bond in the latter conformation might serve to stabilize it.

The GROMACS 3.2.1 trajectory for PTX starting with the polar conformation over an 11 ns time course is displayed in Figure 2. T-Taxol appears at least four times. The fact that this form is not dominant or even strongly populated is consistent with the

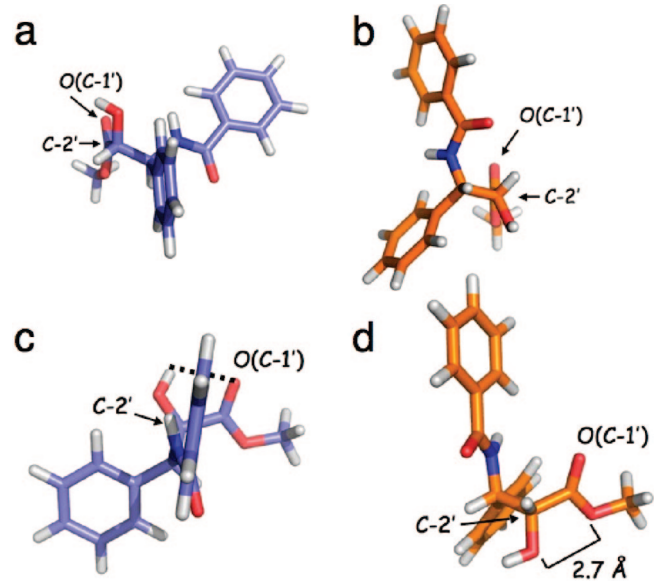

Figure 1. Comparison of the C-13 side chains of T-Taxol and PTX-NY: (a and b) View the two conformations by looking down the C2′−C1′ bond; (c and d) Side views showing a weak internal H-bond for T-Taxol and a repulsive O---O interaction for PTX-NY, respectively.

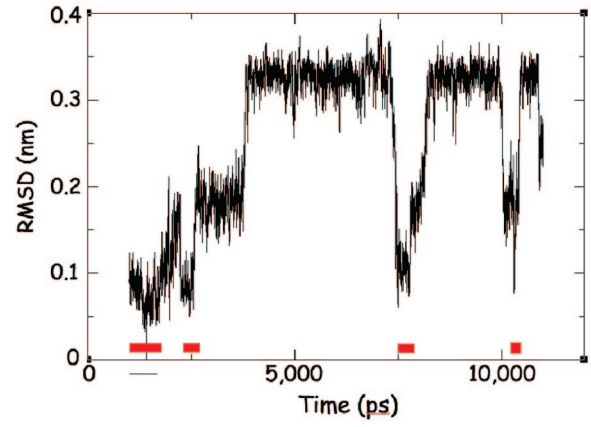

Figure 2. GROMACS 3.2.1 trajectory for PTX over an 11 ns time course. The appearances of T-Taxol are indicated by the red bars.

observation that T-Taxol appears in the solution ensemble of conformations as determined by NMR to the extent of 2−4%, independent of solvent polarity.[19] On the other hand, no examples of PTX-NY could be found. The implication is that along the 300 K trajectory water hydrogen bonding to the C-2′ OH group is insufficient to override the 7.6 kcal/mol energy difference between the two conformations in this force field model (see Experimental Section). From an energy standpoint, a similar situation may apply to a model of PTX-NY sited in the tubulin taxane cleft as well. That is, it may be possible to capture the conformation in a tightly fitting environment displaying a C-2′ OH/His227 H-bond, but in a pose that is nevertheless intrinsically unstable.

***β*-Tubulin Binding Poses for T-Taxol and PTX-NY Conformations.** Can the two conformations under study dock into the *β*-tubulin binding cleft by adopting satisfying binding poses? To examine this question, we employed the 1JFF electron crystallographic refinement of the protein.[14] Initially, the extra precision Glide docking algorithm was applied to four separate PTX conformations (T-Taxol, PTX-NY, and the A and B conformations from the single-crystal X-ray structure[4]), allowing for ligand flexibility, but operating within a static protein.[31] In all four cases, the molecular shapes are docked to give a common conformation; namely, the combined translational and torsional search paths uniformly reshape the ligand to dock it in the T-Taxol conformation.

Thinking that the preorganized binding site might bias the protein-inflexible docking result, we repeated the exercise with the Prime algorithm, which allows for both ligand and protein flexibility.[32] This exercise led to the same result; only T-Taxol poses were predicted with very minor alterations in the binding pocket amino acid side chains. Taken at face value, this implies that the electron crystallographic structure of *β*-tubulin, one that fits very comfortably into the 8 Å resolution structure of microtubules,[33] is incompatible with the PTX-NY conformation.

Part of the problem associated with identifying a ligand-faithful pose for the latter was anticipated by the discussion above around Figures 1a and 1b. Namely, the C-13 terminal phenyl rings reside in substantially different regions of space than those of T-Taxol. The problematic situation is illustrated by the structure of the tubulin−PTX-NY complex derived by the Stony Brook group[34] associated with their original proposal for PTX-NY as the bioactive PTX binding conformation.[22] In order to accommodate the PTX-NY geometry, the short loop connecting *β*-strands B9 and B10 in *β*-tubulin has moved into the binding site, and the backbone residue atoms were displaced from 2 to 4 Å. This pushes the ligand in the direction of the M loop on the opposite side of the binding site. In turn, the M loop is remodeled by as much as 7.5 Å relative to the experimental structures[12,14,15] (backbone atom displacements range from 2 to 7.5 Å). However, the most severe dislocation of tubulin in the Stony Brook structure is helix 1, which is unraveled.[35] Simple superposition of PTX-NY on T-Taxol in the EC tubulin−PTX complex illustrates the situation prior to any binding site reorganization (Figure 3).

The C-13 benzamidophenyl ring experiences a serious steric clash between the aromatic ring and helix H-1, while the C-3′ phenyl is in sub-van der Waals contact with the short loop connecting *β*-sheet strands B9 and B10. This severe molecular crowding is the driving force behind binding site restructuring during attempts to derive a relaxed ligand environment.

To probe this point further, we performed two tests combining MD simulation and geometry optimization to examine the consequences of generating a PTX-NY binding site pose without undue steric interaction with the protein. In the first, the frozen PTX-NY conformer remained in place, while the tubulin protein was allowed to move around it. In the second, the same torsionally frozen conformer was permitted translational freedom during protein movement. Both approaches (see Experimental Section) deliver the same qualitative outcome. Figure 4 (orange) depicts the pose

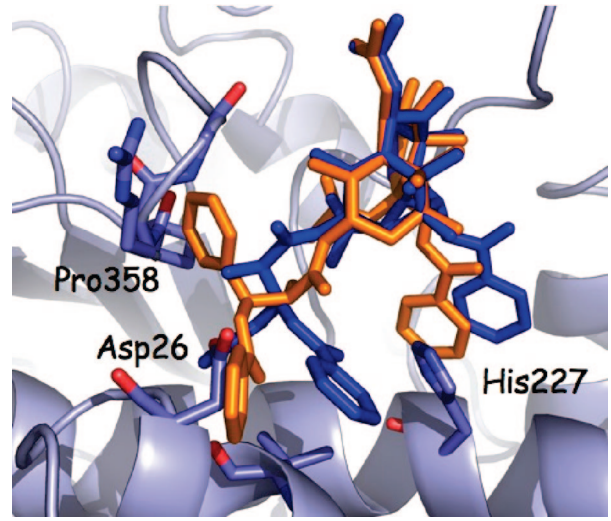

Figure 3. T-Taxol (blue) in *β*-tubulin[14] in which PTX-NY (orange) is superposed by matching atoms in the baccatin core. This placement of PTX-NY leads to severe steric interactions at the head of helix H-1 (Asp26) and at the loop between strands B9 and B10 (Pro358).

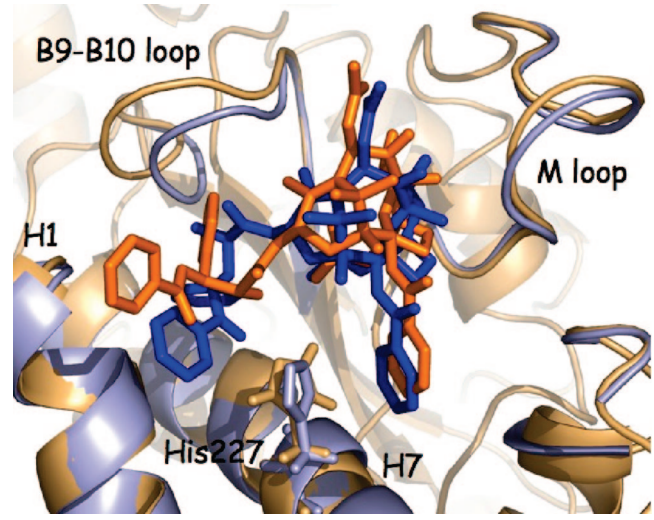

Figure 4. Superposition of T-Taxol (blue) in the EC-determined structure of *β*-tubulin (light blue) and PTX-NY (orange) in the *β*-tubulin binding site (light orange) following elimination of severe steric contacts for the latter (e.g., Figure 1) by MD and geometry optimization.

resulting from the second experiment that retains the PTX-NY geometry but permits ligand translation and protein structure relaxation around the binding site.

Several observations are evident from the optimized structure obtained at the end of the treatment. As mentioned in the Experimental Section, the terminus of H-1 is frayed and the backbone atoms of the B9−B10 loop are displaced on average by 2.3 Å with a maximum displacement of 2.9 Å relative to the location in the electron crystallographic structures. Furthermore, the PTX-NY ligand has been translated upward and out of the binding pocket, exposing the C-3′ benzamido phenyl moiety to solvent. We have commented previously that the C-13 side chain disposition of PTX-NY is incompatible with the EC density by comparison to T-Taxol.[21a,24,25] Structural changes necessary to retain the PTX-NY geometry, while eliminating van der Waals compression as shown in the orange model of Figure 4, are likewise grossly incompatible with the experimental EC density. Other PTX-NY/*β*-tubulin models can certainly arise from different MD treatments,

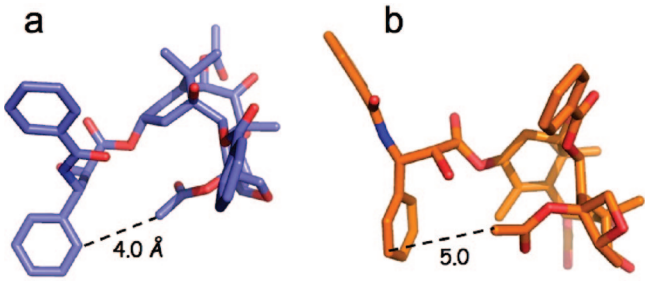

Figure 5. T-Taxol and PTX-NY conformations illustrating the geometric relationship between the C-4 acetate methyl and *ortho*-position of the C-13 phenyl rings. (a) T-Taxol; the methyl and ring are in a common plane ((C4OAc)C---C−C(C13)−C improper torsion is 179°). (b) PTX-NY; the methyl group is above and orthogonal to the face of the phenyl ring ((C4OAc)C---C−C(C13)−C, 95°).

as indicated by the differences between the PTX-NY Stony Brook model and our own. However, as long as the PTX-NY conformation is enforced, the surrounding tubulin protein binding site must deform to accommodate it. Such models are likewise subject to violation of the experimental constraints imposed by the measured EC density.

It should be added that previous docking of PTX-NY into β-tubulin not only recognized the necessity for reorganization of side chains at the protein binding site, but viewed it as an asset, a type of "partial induced fit".[22] This viewpoint has merit in circumstances where the transformation takes place from the apoprotein to the bound form, or where a significantly modified member of a ligand family exhibits a binding pose that varies significantly from the parent ligand. Its validity is highly questionable, however, when a ligand is manipulated to assume a docking pose by altering the location of the surrounding side chains for a protein that has already been solved with the same ligand in the same binding site. In the present case, Figures 3 and 4 illustrate the dichotomy between the experimental solution to the binding of PTX to β-tubulin and an alternative virtual solution.

Design of Taxanes More Potent than PTX. Bridged taxanes designed on the basis of T-Taxol, but not other conformations,[28] have been unique in delivering analogues with 20−50-fold greater cytoxicity than parent PTX.[16,17] The basis for the design is illustrated in Figure 5, which compares the spatial association of the C-4 acetate methyl group and the *ortho*-carbon of the C-13 phenyl, the two centers connected by the two-carbon bridges in **2** and **3**. Not only is this distance shorter for T-Taxol, but its geometry is compatible with the expectation that a short bridge would retain the original conformation. That is, the improper dihedral angle (C4OAc)C---C−C(C13)−C is 179°, placing the H atoms to be replaced by linker carbons in or near a common plane consistent with the geometries of **2** and **3**. For example, the interatomic distances for the latter global minima optimized by MMFFs[24] are 3.7 and 3.9 Å, respectively, nearly identical to the distance in Figure 5a. Equally satisfying, the (C4OAc)C---C−C(C13)−C improper torsions are 157° and 160°, respectively. PTX-NY, on the other hand, positions the C-4 acetate methyl group 5 Å above and orthogonal to the plane of the C-13 phenyl ring ((C4OAc)C---C−C(C13)−C, 95°), as illustrated by Figure 5b. Such an orientation does not suggest introduction of a bridge between the key carbons unless the C-13 phenyl is twisted into a sterically unfavorable rotamer, as quantified by Tables 6−8. At the same time, the PTX-NY methyl to π-face geometry anticipates a significant torsional reorganization upon bridge installation (cf. Figures 1a and 1b). T-Taxol is clearly the superior molecular shape for predicting T-constrained molecules such as **2** and **3**.

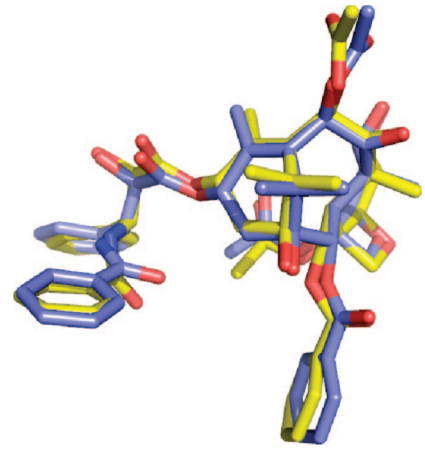

Figure 6. PTX-bound conformations extracted from the superposed tubulin−PTX complexes derived from the experimental EC density; T-Taxol (blue),[15] 1JFF (yellow).[14]

Conclusions

The T-Taxol conformation was first observed as a <4% population conformation for PTX in $CDCl_3$,[26] but it proved to satisfy the density derived from two independent treatments of a 3.5 Å resolution electron crystallographic (EC) analysis of the tubulin−paclitaxel complex (Figure 6).[14,15]

Nonetheless, the Ojima group, having previously proposed two conformationally distinct PTX structures as the bioactive form bound to β-tubulin,[36−38] suggested a third option, PTX-NY, and presented it as an alternative to the T-Taxol conformer.[22,23] Comparisons of T-Taxol and PTX-NY conformations with respect to the tubulin−PTX $2F_{obs} - F_{calc}$ density omit maps illustrate clearly that the C-13 side chain of the latter conformer is well outside the experimental density contour.[21a,24,25] The present work provides four additional reasons for disbelieving that PTX-NY represents the 3-D shape of paclitaxel bound to β-tubulin.

First, the energies of the PTX-NY conformation both for parent PTX and highly active bridged analogues **2** and **3** are estimated to be 3−28 kcal/mol higher than those of T-Taxol, with an average $\Delta\Delta E$ of 11 kcal/mol across 34 separate energy evaluations (Tables 2−8). The generalization applies to both the truncated C-13 side chain and full taxane structures in both molecular mechanics and quantum chemical frameworks (Tables 2−8). Such high-energy forms might be worth considering, if T-Taxol were to evidence any structural or biological liabilities with respect to its interaction with β-tubulin. It does not. Second, an 11 ns molecular dynamics trajectory for PTX at 300 K in a pool of explicit water molecules reveals the presence of T-Taxol at a few points along the path. This is consonant with the existence of this conformation in solution to the extent of 2−4%.[19] The absence of PTX-NY along the same pathway conforms to the high energy of this conformer by comparison. Third, the PTX-NY geometry is not easily fitted into the β-tubulin binding pocket derived from electron crystallography. However, the extreme steric clashes can be relieved by reconstructing the protein binding site and translating the ligand to a more favorable location. Unfortunately, the resulting pose is no longer faithful to the experimental data. Fourth, the T-Taxol geometry has been extraordinarily successful in designing annular taxanes that show large cytotoxicity enhancements relative to parent PTX. No other bridging principle of the many attempted[28] has achieved this feat. The 3D constitution of PTX-NY (Figure 5b) is unsuitable for projecting structures such as **2** and **3**, while extension of the T-Taxol shape (Figure 5a) provides them naturally. Other similar analogues are possible and may prove their merit in the future.

Experimental Section

General Experimental Procedures. The molecular mechanics and molecular dynamics computations described below were performed with the Maestro 8.5.111 software suite,[39] the GROMOS96.1 force field,[40]

and the OpenEye[41] ROCS (Rapid Overlay of Chemical Structures) 3-D shape-based similarity perception package[26] installed on a series of Linux computers. The quantum chemical density functional energies were obtained with the Gaussian 03 suite of programs[42] operating on IBM Power4+ processors.

C-13 Side Chain Conformational Analysis. The T-Taxol and PTX-NY[34] C-13 side chains were excised from the full taxane structures to include the C-13 carbon, which was converted to a methyl group. The corresponding side chains with all torsions restrained to their original values were optimized with both MMFFs and OPLS-2005 force fields in Maestro 8.5.111.

To determine if both T-Taxol and PTX-NY C-13 side chain conformers are energy minima on the molecular mechanics energy surfaces, conformational searches for **5** with geometry optimization were performed using both MMFFs and OPLS-2005 force fields with the mixed Monte Carlo and Low Mode methods in Maestro 8.5.111. Employing 10 000 steps and an energy cutoff of 10 kcal/mol, the global minima were found 200 and 28 times, respectively, assuring that the searches were complete.[43] The resulting structures were further optimized to convergence and filtered for duplicates, giving 102 and 101 unique conformations, respectively. With the MMFFs and OPLS-2005 optimized structures (Table 1) as templates, the 3-D shape-based searching tool ROCS[27] was used to locate each structure in each conformational pool. The T-Taxol side chain proved to be 1.8 and 0.4 kcal/mol above the global minima, respectively, while the PTX-NY side chain was found 6.5 and 8.4 kcal/mol above the same global minima, respectively.

The OPLS-2005 constrained-optimized structures of both side chains (Table 1) were imported into Gaussian03,[42] and single-point calculations were performed using HF (with basis sets 6-31G*, 6-311G*, and 6-311+G*), B3LYP (6-31G*, 6-311G*, and 6-311+G*), and MP2 (6-31G*, 6-311G*, and 6-311+G*). The resulting energies and differences are provided in Table 2.

Energy Comparisons for Full T-Taxol and PTX-NY Structures. Both T-Taxol and PTX-NY initial starting structures were optimized with full torsional constraints using the following force fields: MM2, MMFFs, OPLS-2001, OPLS-2005, and OPLS-2005/MMFFs. Subsequently, each of the structures was optimized without constraints to the nearest local minima employing the same set of force fields. The energy results are provided in Tables 3 and 4, respectively.

Single-point energies using several Gaussian03-based quantum chemical models were calculated for the T-Taxol and PTX-NY geometries obtained by sequential torsion-constraint optimization with the OPLS-2005 and MMFFs force fields as given in the last entry of Table 3. Table 5 lists the models employed and the energy comparisons.

Bridged Taxanes 2 and 3. Structures of **2** and **3** in T-Taxol conformations (T-Taxol-**2** and T-Taxol-**3**, respectively) were those employed in a previously reported molecular dynamics study.[18] The structures of conformers **2** and **3** in PTX-NY conformations (PTX-NY-**2** and PTX-NY-**3**, respectively) were produced by introducing the linkers into a tubulin−PTX-NY complex[34] using Maestro 8.5.111 followed by energy minimization using the OPLS-2005 force field, a distance-dependent dielectric, and the GBSA/H_2O continuum solvation model. The backbone of the protein was fixed throughout the energy minimizations. As with parent PTX (Tables 3 and 4), the bridged conformers resulting from the latter treatment were energy-minimized without constraints using a variety of force fields (Tables 6 and 7). All of the protein-free bridged structures obtained in this way remain in the PTX-NY conformation.

As for the unbridged parent PTX conformations, single-point energies using several Gaussian03-based quantum chemical models were calculated for **2** and **3** with T-Taxol and PTX-NY geometries obtained by sequential torsion-constraint optimization with the OPLS-2005 and MMFFs force fields as given in the last entries of Table 6 and 7. Table 8 lists the models employed and the energy comparisons.

Molecular Dynamics (MD) for T-Taxol and PTX-NY in Water. As a preliminary to analyzing the molecular dynamics trajectory for PTX with the GROMOS96.1 force field,[40] we obtained the method's estimate of ΔE between T-Taxol and PTX-NY. Thus, energies of the OPLS-2005/MMFFs constrained geometries were calculated as single points to give an energy difference favoring T-Taxol by 31.6 kJ/mol (7.6 kcal/mol), entirely consistent with the range of values predicted by other force fields (Table 3).

Previously, we reported a molecular dynamics analysis for PTX and several bridged analogues performed with GROMACS 3.2.1.[18] For PTX, the polar conformation[4,21b,44] was solvated in a box of 512 SPC water molecules and subjected to 11 ns of MD at 300 K with a time step of 1 fs under NPT conditions. Examination of the MD trajectory by comparing the overall rmsd for PTX relative to T-Taxol over the 11 ns time course of the simulation revealed that, while the molecule assumes many different conformations, the T-form is sampled at least four times. In the present work, a similar analysis was performed for PTX-NY. Since the overall rms deviation between T-Taxol and PT-NY is small (1.8 Å), explicit examination of structures along the trajectory segments expected to contain the two forms was carried out. The PTX-NY conformation did not appear among the structures.

Docking of T-Taxol and PTX-NY in β-Tubulin. The PTX ligand in β-tubulin (pdb code 1JFF) was removed, and the protein was "prepared" in Maestro 8.5.111[39] by adding hydrogens, assigning bond orders, and subjecting the structure to 200 steps of optimization applied to nonbonded interactions with OPLS-2005. Subsequently, an extra precision flexible Glide[31] docking was performed using T-Taxol, PTX-NY, and the two conformers determined in the single-crystal X-ray structure (A (extended) and B (polar)).[4] All four structures result in T-Taxol variants as the most favored Glide pose. In no case did PTX-NY appear as a solution to the docking problem.

Extra precision induced-fit docking with Prime[32] in Maestro 8.5.111 explores flexibility of both the ligand and the protein side chains in the target region of the selected protein. The protocol was utilized to compare any possible reorganization of the binding site that might better accommodate the PTX-NY conformation. However, the latter, like T-Taxol, docks with very little reorganization of protein side chains to deliver the T-Taxol bound conformation once again.

To develop a model of PTX-NY in β-tubulin, initially the baccatin core of PTX-NY was superposed on that of T-Taxol in the 1JFF binding site, resulting in the terminal C-13 benzamido phenyl and phenyl moieties residing in somewhat different and significantly different locations in the pocket, respectively (Figure 3). The benzamido phenyl makes contacts well below the sum of atomic van der Waals radii with Asp26 and helix H-1, while the C-3′ phenyl makes similar contacts with residues along the short loop connecting β-strands B9 and B10, in particular Pro358.

Two different strategies were employed to develop ligand−protein binding models to accommodate the PTX-NY conformation without violating the usual van der Waals restraints. The first strategy locked the torsion-constrained PTX-NY ligand in place, but permitted all residues in the binding site within 8 Å of ligand atoms to move at 20 K for 1000 fs (Tripos force field,[45] Pullman charges, 0.5 fs step, NTV, dielectric constant 4.5). This was followed by 500 steps of optimization, MD at 50 K for another 1000 fs, a second 500 steps of optimization, MD at 300 K for 1000 fs, and finally 1000 steps of optimization. In the second strategy, the torsions of the ligand were constrained to those of PTX-NY, but the ligand was allowed translational motion under the same conditions of MD and optimization as those described for the first strategy.

The binding site arising from the first strategy experiences a displacement of the B9−B10 loop near the C-3′ phenyl and fraying of the end of helix H-1 that sits against the benzamide phenyl. In the binding site from the second strategy, the ligand moves to avoid unfavorable contacts with the protein. Consequently, the benzamido phenyl ring shifts slightly further out of the pocket. Again, the terminus of H-1 is somewhat frayed and the B9−B10 loop moves away from the ligand to open up the binding site (Figure 4). In neither of these models is there significant H-bonding between the C2′-OH group and His227, although more extensive MD might sample such an interaction.

Acknowledgment. This work has been generously supported by NIH grant CA-69571. We are likewise grateful to M. Geballe (Emory University) and D. Kingston (Virginia Polytechnic Institute and State University) for many helpful discussions, and to the OpenEye Scientific Software group for their generous provision of ROCS. D. Liotta (Emory University) is greatly appreciated for his constant support of our efforts.

Note Added after ASAP Publication: Bristol-Myers was changed to NCI in the first sentence in the version posted on March 27, 2009.

Supporting Information Available: Atomic coordinates for T-Taxol and PTX-NY are available free of charge via the Internet at http://pubs.acs.org.

References and Notes

(1) Goodman, J.; Walsh, V. *The Story of Taxol: Nature and Politics in the Pursuit of an Anti-Cancer Drug*; Cambridge University Press: Cambridge, UK, 2001.

(2) Wani, M. C.; Taylor, H. L.; Wall, M. E.; Coggon, P.; McPhail, A. T. *J. Am. Chem. Soc.* **1971**, *93*, 2325–2327.
(3) Schiff, P. B.; Fant, J.; Horwitz, S. B. *Nature* **1979**, *277*, 665–667.
(4) Mastropaolo, D.; Camerman, A.; Luo, Y.; Brayer, G. D.; Camerman, N. *Proc. Natl. Acad. Sci. U.S.A.* **1995**, *92*, 6920–6924.
(5) Interestingly, although ref 4 reports that atomic coordinates of the two conformations of PTX found in the ligand-only single-crystal X-ray study were to be deposited in the Cambridge Crystallographic Database, the coordinates have never been made available to the community.
(6) http://en.wikipedia.org/wiki/Taxol. Accessed 12/27/08.
(7) (a) Scripture, C. D.; Figg, W. D.; Sparreboom, A. *Curr. Neuropharmacol.* **2006**, *4*, 165–172. (b) Kuppens, I. E. *Curr. Clin. Pharmacol.* **2006**, *1*, 57–70.
(8) Giannakakou, P.; Snyder, J. P. In *Tubulin and Microtubules*; Fojo, T., Ed.; Humana Press: Totowa, NJ, 2008.
(9) (a) Perez, E. A. *Breast Cancer Res. Treat.* **2008**, Dec 20, Epub ahead of print. . (b) Mooberry, S. L. *Methods Mol. Med.* **2007**, *137*, 289–302.
(10) http://www.cptech.org/ip/health/taxol/. Accessed 12/27/08.
(11) (a) Rao, S.; Krauss, N. E.; Heerding, J. M.; Orr, G. A.; Horwitz, S. B. *J. Biol. Chem.* **1994**, *269*, 3132–3134. (b) Combeau, C.; Commerçon, A.; Mioskowski, C.; Rousseau, B.; Aubert, F.; Goeldner, M. *Biochemistry* **1994**, *33*, 6676–6683. (c) Rao, S.; Orr, G. A.; Chaudhary, A. G.; Kingston, D. G. I.; Horwitz, S. B. *J. Biol. Chem.* **1995**, *270*, 20235–20238. (d) Rao, S.; He, L.; Chakravarty, S.; Ojima, I.; Orr, G. A.; Horwitz, S. B. *J. Biol. Chem.* **1999**, *274*, 37990–37994.
(12) Nogales, E.; Wolf, S. G.; Downing, K. H. *Nature* **1998**, *391*, 199–203.
(13) For an overview of the application of electron crystallography to microtubule stabilizing agents including PTX, cf. Nettles, J. H.; DowningK. H. In *Tubulin-Binding Agents: Synthetic, Structural and Mechanistic Insights*; Carlomagno, T., Ed.; Topics in Current Chemistry, Vol. 286; Springer: Berlin, 2008, in press.
(14) Lowe, J.; Li, H.; Downing, K. H.; Nogales, E. *J. Mol. Biol.* **2001**, *313*, 1045–1057.
(15) Snyder, J. P.; Nettles, J. H.; Cornett, B.; Downing, K. H.; Nogales, E. *Proc. Natl. Acad. Sci. U.S.A.* **2001**, *98*, 5312–5316.
(16) Ganesh, T.; Guza, R. C.; Bane, S.; Ravindra, R.; Shanker, N.; Lakdawala, A. S.; Snyder, J. P.; Kingston, D. G. I. *Proc. Nat. Acad. Sci. U.S.A.* **2004**, *101*, 10006–10011.
(17) Ganesh, T.; Yang, C.; Norris, A.; Glass, T.; Bane, S.; Ravindra, R.; Banerjee, A.; Metaferia, B.; Thomas, S. L.; Giannakakou, P.; Alcaraz, A. A.; Lakdawala, A. S.; Snyder, J. P.; Kingston, D. G. I. *J. Med. Chem.* **2007**, *50*, 713–725.
(18) Shanker, N.; Kingston, D. G. I.; Ganesh, T.; Yang, C.; Alcaraz, A. A.; Geballe, M. T.; Banerjee, A.; McGee, D.; Snyder, J. P.; Bane, S. *Biochemistry* **2007**, *46*, 11514–11527.
(19) In D_2O/DMSO-d_6 or $CDCl_3$, PTX presents the T-Taxol form with populations of 2% and 4%, respectively; cf. ref 16.
(20) Querolle, O.; Dubois, J.; Thoret, S.; Roussi, F.; Guéritte, F.; Guénard, D. *J. Med. Chem.* **2004**, *47*, 5937–5944.
(21) (a) Paik, Y.; Yang, C.; Metaferia, B.; Tang, S.; Bane, S.; Ravindra, R.; Shanker, N.; Alcaraz, A. A.; Johnson, S. A.; Schaefer, J.; O'Connor, R. D.; Cegelski, L.; Snyder, J. P.; Kingston, D. G. I. *J. Am. Chem. Soc.* **2007**, *129*, 361–370. (b) Li, Y.; Poliks, B.; Cegelski, L.; Poliks, M.; Gryczynski, Z.; Piszczek, G.; Jagtap, P. G.; Studelska, D. R.; Kingston, D. G. I.; Schaefer, J.; Bane, S. *Biochemistry* **2000**, *39*, 281–291.
(22) Geney, R.; Sun, L.; Pera, P.; Bernacki, R. J.; Xia, S.; Horwitz, S. B.; Simmerling, C. L.; Ojima, I. *Chem. Biol.* **2005**, *12*, 339–348.
(23) Sun, L.; Geng, X.; Geney, R.; Li, Y.; Simmerling, C.; Li, Z.; Lauher, J. W.; Xia, S.; Horwitz, S. B.; Veith, J. M.; Pera, P.; Bernacki, R. J.; Ojima. I. *J. Org. Chem.* **2008**, DOI: 10.1021/jo801713q.
(24) Alcaraz, A. A.; Mehta, A. K.; Johnson, S. A.; Snyder, J. P. *J. Med. Chem.* **2006**, *49*, 2478–2488.
(25) Johnson, S. A.; Alcaraz, A.; Snyder, J. P. *Org. Lett.* **2005**, *7*, 5549–5552.
(26) Snyder, J. P.; Nevins, N.; Cicero, D. O.; Jansen, J. *J. Am. Chem. Soc.* **2000**, *122*, 724–725.
(27) (a) Rush, T. S.; Grant, J. A.; Mosyak, L.; Nicholls, A. *J. Med. Chem.* **2005**, *48*, 1489–1494. (b) Hawkins, P. C. D.; Skillman, A. G.; Nicholls, A. *J. Med. Chem.* **2007**, *50*, 74–82.
(28) Kingston, D. G. I.; Bane, S.; Snyder, J. P. *Cell Cycle* **2005**, *4* (2), 279–289.
(29) Matesanz, R.; Barasoain, I.; Yang, C.-G.; Wang, L.; Li, X.; de Ines, C.; Coderch, C.; Gago, R.; Barbero, J. J.; Andreu, J. M.; Fang, W.-S.; Diaz, J. F. *Chem. Biol.* **2008**, *15*, 573–585.
(30) Bondi, A. *J. Phys Chem.* **1964**, *68*, 441–451.
(31) (a) Friesner, R. A.; Banks, J. L.; Murphy, R. B.; Halgren, T. A.; Klicic, J. J.; Mainz, D. T.; Repasky, M. P.; Knoll, E. H.; Shaw, D. E.; Shelley, M.; Perry, J. K.; Sander, L. C.; Shenkin, P. S. *J. Med. Chem.* **2004**, *47*, 1739–1749. (b) Halgren, T. A.; Murphy, R. B.; Friesner, R. A.; Beard, H. S.; Frye, L. L.; Pollard, W. T.; Banks, J. L. *J. Med. Chem.* **2004**, *47*, 1750–1759.
(32) Zhu, K.; Shirts, M. R.; Friesner, R. A. *J. Chem. Theory Comput.* **2007**, *3*, 2108–2119.
(33) Li, H.; DeRosier, D. J.; Nicholson, W. V.; Nogales, E.; Downing, K. H. *Structure* **2002**, *10*, 1317–1328.
(34) The atomic coordinates of the PTX-NY ligand structure embedded in a partial β-tubulin protein structure generated by the two-step covalent/noncovalent procedure of ref 22 were kindly provided by Professor Iwao Ojima (State University of New York, Stony Brook, NY).
(35) Since helix H-7 of the partial protein structure displays correct secondary structure, the pdb file has been correctly read and interpreted.
(36) Ojima, I.; Kuduk, S. D.; Chakravarty, S.; Ourevitch, M.; Begue, J.-P. *J. Am. Chem. Soc.* **1997**, *119*, 5519–5527.
(37) Ojima, I.; Inoue, T.; Chakravarty, S. *J. Fluor. Chem.* **1999**, *97*, 3–10.
(38) Ojima, I.; Chakravarty, S.; Inoue, T.; Lin, S.; He, L.; Horwitz, S. B.; Kuduk, S. C.; Danishefsky, S. J. *Proc. Natl. Acad. Sci.* **1999**, *96*, 4256–426.
(39) Schrödinger, Inc., 101 SW Main Street, Suite 1300, Portland, OR 97204; http://www.schrodinger.com/ProductDescription.php?mID=6&sID=15&cID=0.
(40) van Gunsteren, W. F.; Billeter, S. R.; Eising, A. A. ; Hünenberger, P. H. ; Krüger, P.; Mark, A. E.; Scott, W. R. P. ; Tironi, I. G. *Biomolecular Simulations: The GROMOS96 manual and user guide*; Vdf Hochschulverlag: ETH Zürich, Switzerland, 1996.
(41) OpenEye Scientific Software, 9 Bisbee Court, Suite D, Santa Fe, NM 87508; http://www.eyesopen.com/.
(42) Frisch, M. J. ; Trucks, G. W.; Schlegel, H. B.; Scuseria, G. E.; Robb, M. A.; Cheeseman, J. R.; Montgomery, Jr., J. A.; Vreven, T.; Kudin, K. N. ; Burant, J. C.; Millam, J. M.; Iyengar, S. S.; Tomasi, J.; Barone, V.; Mennucci, B.; Cossi, M.; Scalmani, G.; Rega, N.; Petersson, G. A.; Nakatsuji, H.; Hada, M.; Ehara, M.; Toyota, K.; Fukuda, R.; Hasegawa, J.; Ishida, M.; Nakajima, T.; Honda, Y.; Kitao, O.; Nakai, H.; Klene, M.; Li, X.; Knox, J. E.; Hratchian, H. P.; Cross, J. B.; Bakken, V.; Adamo, C.; Jaramillo, J.; Gomperts, R.; Stratmann, R. E.; Yazyev, O.; Austin, A. J.; Cammi, R.; Pomelli, C. ; Ochterski, J. W.; Ayala, P. Y.; Morokuma, K.; Voth, G. A.; Salvador, P. ; Dannenberg, J. J.; Zakrzewski, V. G.; Dapprich, S.; Daniels, A. D.; Strain, M. C.; Farkas, O.; Malick, D. K.; Rabuck, A. D.; Raghavachari, K.; Foresman, J. B.; Ortiz, J. V.; Cui, Q.; Baboul, A. G.; Clifford, S.; Cioslowski, J.; Stefaznov, B. B.; Liu, G. ; Liashenko, A.; Piskorz, P.; Komaromi, I.; Martin, R. L.; Fox, D. J.; Keith, T.; Al-Laham, M. A.; Peng, C. Y.; Nanayakkara, A.; Challacombe, M.; Gill, P. M. W.; Johnson, B.; Chen, W.; Wong, M. W.; Gonzalez, C.; Pople, J. A. *Gaussian 03, Revision C.02*; Gaussian, Inc.: Wallingford, CT, 2004.
(43) Chang, G.; Guida, W. C.; Still, W. C. *J. Am. Chem. Soc.* **1989**, *111*, 4379–4386.
(44) Vander Velde, D. G.; Georg, G. I.; Grunewald, G. L.; Gunn, C. W.; Mitscher, L. A. *J. Am. Chem. Soc.* **1993**, *115*, 11650–11651.
(45) (a) Clark, M.; Cramer, R. D.; Van Opdenbosch, N. *J. Comput. Chem.* **1989**, *10*, 982–1012. (b) (cf. http://www.tripos.com/. Accessed 12/27/08).

NP800662J